MAC in Motion: Impact of Mobility on the MAC of Drive-Thru Internet

Tom H. Luan, Xinhua Ling, and Xuemin (Sherman) Shen, *Fellow*, *IEEE*

Abstract—The pervasive adoption of IEEE 802.11 radios in the past decade has made possible for the easy Internet access from a vehicle, notably drive-thru Internet. Originally designed for the static indoor applications, the throughput performance of IEEE 802.11 in the outdoor vehicular environment is, however, still unclear especially when a large number of fast-moving users transmitting simultaneously. In this paper, we investigate the performance of IEEE 802.11 DCF in the highly mobile vehicular networks. We first propose a simple yet accurate analytical model to evaluate the throughput of DCF in the large scale drive-thru Internet scenario. Our model incorporates the high-node mobility with the modeling of DCF and unveils the impacts of mobility (characterized by node velocity and moving directions) on the resultant throughput. Based on the model, we show that the throughput of DCF will be reduced with increasing node velocity due to the mismatch between the MAC and the transient high-throughput connectivity of vehicles. We then propose several enhancement schemes to adaptively adjust the MAC in tune with the node mobility. Extensive simulations are carried out to validate the accuracy of the developed analytical model and the effectiveness of the proposed enhancement schemes.

Index Terms—Vehicular networks, mobility, distributed coordination function (DCF), embedded Markov chain.

1 Introduction

While communication and especially the connectivity to the Internet has become an essential part of our daily life, high-rate Internet access from vehicles is still a luxury in most areas. Using the traditional wireless communications, e.g., cellular or satellite communications, with the need to provide ubiquitous coverage to a large population of users, the available data rate for each user is far from enough to deliver the media-rich Internet contents. Moreover, Americans are reported [1] to spend up to 540 hours on average a year in their vehicles, and collectively almost a billion "commuter hours" a week in automobiles. That is to say, in nearly 10 percent of the waking time, people would have very limited or even no Internet access at all.

Catering to the ever-increasing demand, the vehicular network has recently been introduced to provide the high rate yet cheap Internet access to vehicles by utilizing the "grass root" IEEE 802.11 access points (APs) deployed along the roads. An example is shown in Fig. 1. Ott and Kutscher [2] first report the real-world measurements between a moving car with an external antenna and roadside Wireless LAN AP, namely drive-thru Internet. They show that using the off-the-shelf IEEE 802.11b hardware, a vehicle could maintain a connection to a roadside AP for around 500 m and transfer 9 MB of data at 80 km/h using either TCP or UDP. CarTel in MIT [3] further extends the drive-thru Internet with city-wide trials in Boston and reports the upload bandwidth available to vehicles using the unplanned open residential APs. It is shown that the plethora IEEE 802.11b APs deployed in cities could provide vehicle nodes with the *intermittent* and *short-lived* connectivity, yet high throughput when the connectivity is available. Similar properties of the drive-thru Internet are also reported separately in [4], [5]. Meanwhile, prominent automobile corporations have also lunched important projects using the similar architecture for promoting vehicular Internet communications. For instance, Mercedes-Benz proposes to deploy the "InfoFuel" stations along the roads to fuel on-road vehicles with the high-throughput Internet access using the IEEE 802.11a radio [6].

While being seriously pursued, the performance of IEEE 802.11 in the *high-speed large-scale* drive-thru Internet scenario is still unclear due to the following reasons. *First*, compared with the small-scale indoor scenarios, the drive-thru Internet is typically a much larger network composed of tens or hundreds of users. Previous works in [2], [3], [4], [5] largely adopt the experimental approach; limited by the hardware, their results are attained in small-scale networks only and can hardly provide insights into the large-scale case when a great number of vehicles compete for communications simultaneously. Therefore, we argue that a thorough theoretical framework which is accurate and scalable to different network scales is necessary to guide the real-world deployments. *Second*, originally designed for low-mobility scenarios, the IEEE 802.11 adopts the contention-based distributed coordination function (DCF) as its MAC in which the transmission opportunity of stations are rendered in an opportunistic manner (refer to Section 2 for details). In the case of drive-thru Internet, as vehicles have volatile connectivity due to the fast mobility, whether DCF can fully utilize the cherished access time of users and provide them the guaranteed throughput is questionable. As the previous theoretical studies on DCF [7], [8] mainly focus on the static WLAN scenarios *without taking the node*

- *T.H. Luan and X. Shen are with the Broadband Communication Research Group, Department of Electrical and Computer Engineering, University of Waterloo, 200 University Avenue West, Waterloo, ON N2L 3G1, Canada. E-mail: hluan@uwaterloo.ca, xshen@bbcr.uwaterloo.ca.*
- *X. Ling is with Research In Motion, 295 Phillip Street, Waterloo, ON N2L 3W8, Canada. E-mail: xling@rim.com.*

Manuscript received 16 Mar. 2010; revised 9 Oct. 2010; accepted 10 Jan. 2011; published online 9 Feb. 2011.
For information on obtaining reprints of this article, please send e-mail to: tmc@computer.org, and reference IEEECS Log Number TMC-2010-03-0127. Digital Object Identifier no. 10.1109/TMC.2011.36.

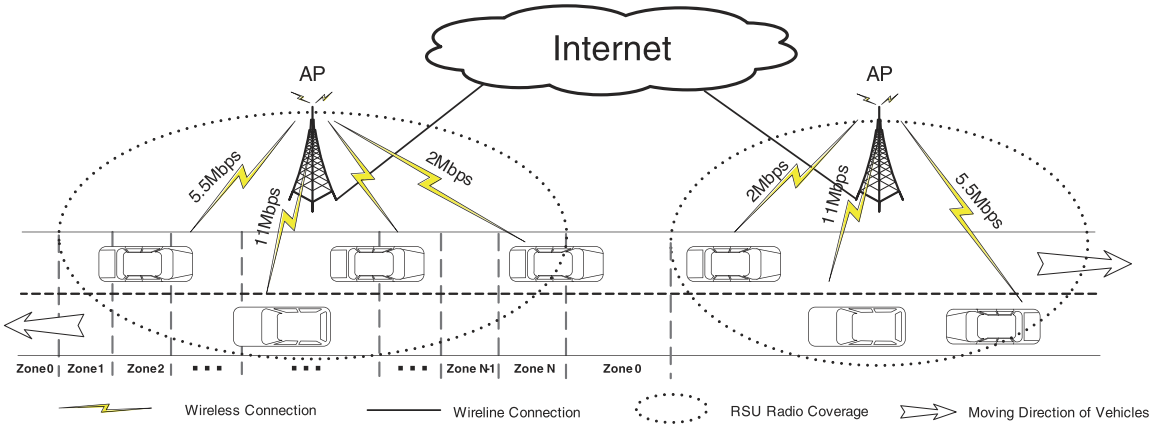

Fig. 1. Drive-thru Internet in which the radio coverage of AP is divided into multiple zones according to the data modulation rates.

mobility into consideration, they are not applicable to the drive-thru Internet scenario.

In this paper, we focus on the DCF performance by considering high-node mobilities. Particularly, we aim at addressing the following questions: *how the performance of DCF is in the high-speed large-scale drive-thru Internet; in what fashion the mobility affects the MAC throughput and, more importantly, how to remedy that*? On addressing these issues, we provide a systematic and theoretical treatment based on a Markov chain model which incorporates the mobility of vehicles in the analysis of DCF. Based on the Markov model, we unveil the impacts of mobility (characterized by the node velocity and moving direction) on the resultant system throughput and describe the optimal configuration of DCF to mitigate the negative effects of mobility toward best system performance. Our main contributions are two-fold:

- *Performance Evaluation*: We propose an accurate and scalable model to analytically evaluate the impacts of node mobility on the achievable system throughput in drive-thru Internet scenarios. The accuracy of the analytical model is demonstrated by extensive simulations. Moreover, we show that the throughput performance is solely dependent on the node velocity. Since velocity can be easily measured, vehicles are able to conveniently assess their throughput with local information only and then optimize the MAC in a fully distributed manner.
- *Protocol Enhancement*: Based on the developed model, we propose to further enhance the MAC throughput by adaptively adjusting the MAC in tune with the node mobility. In particular, we propose three guidelines of the DCF design in the highly mobile vehicular environment, and describe the optimal schemes to determine the channel access opportunity to fully utilize the transient connectivity of vehicles.

The remainder of this paper is organized as follows: we first provide an overview of DCF in Section 2 and discuss the problems when directly implementing it in vehicular communications. Section 3 describes the proposed analytical model in detail and Section 4 validates the accuracy of the analytical model using simulations. In Section 5, we discuss how to boost the performance of DCF by accommodating the high mobility of nodes. Section 6 compares our work with that from the existing literature and Section 7 closes the paper with conclusions.

2 DCF in the Drive-Thru Internet

Using DCF, each node with packets to transmit monitors the availability of the channel. If the channel is sensed idle for a period of distributed interframe space (DIFS), the transmission may proceed; otherwise, the node will wait until the end of the in-progress transmission. To avoid the case that multiple nodes transmit simultaneously when the channel is released idle, DCF adopts the collision avoidance (CA) mechanism. Specifically, before transmission, each node uniformly selects a random discrete backoff time from the range $[0, W-1]$, where W is called the Contention Window (CW). To transmit packets after DIFS, a node first reduces the backoff time with constant step δ, and transmits only if the backoff time is 0. The countdown of backoff time is frozen once the channel becomes busy due to other node transmission, and resumes until the channel is idle for another DIFS. The size of CW, W, depends on the history of transmissions. At the first transmission attempt, W is set to a predefined value CW_{min}, the *minimum contention window*. Upon each unsuccessful transmission s, W is updated as $W = 2^s CW_{min}$ until W reaches a maximum value CW_{max}. s here is called backoff stage. More details of DCF can be found in [9].

The advantages of DCF are salient: *First*, it is fully distributed, which is particularly desirable in vehicular communications. As frequent handoffs and topology changes are made due to the high-node mobility, the distributed behavior of DCF makes the system quite robust. *Second*, thanks to the binary exponential backoff, DCF is scalable and could be implemented for different traffic and road environments, e.g., urban and rural regions.

However, originally designed for stationary indoor networks, when used for the in-motion vehicular communications, the performance of DCF highly depends on the mobility of nodes, as we show in the following sections.

Moreover, with nodes at different locations to an AP, their channel conditions diverse, resulting in different data rates for reliable transmissions, as shown in Fig. 1. In this case, DCF suffers from the *performance anomaly*, i.e., the system throughput is throttled to the minimum transmission rate among nodes [10]. To boost the throughput performance, existing literatures [11], [12], [13] largely

TABLE 1
Summary of Notations

Symbols Associated with Zones and Vehicle Traffic	
$\mathbb{Z}$	Set of spatial zones in the coverage of an AP. z is an element in $\mathbb{Z}$.
r_z	Payload transmission rate (in Mbps) of vehicle node to AP at zone z.
d_z	Length of the spatial zone z (in meters).
λ	Mean arrival rate of vehicles to the road segment.
v	Mean velocity of vehicles (in km/h) in the road segment.
n_L	Number of lanes in the road segment.
k	Density of vehicles (in veh/km/lane) along the road segment.
k_{jam}	Traffic jam density (in veh/km/lane) at which the traffic flow comes to a halt.
v_f	Free-flow speed (in km/h).
Symbols Associated with Transmissions and Backoffs	
W_z	The minimum contention window size $CW_{\min}$ associated in zone z.
m	The maximum backoff stage.
τ_z	Conditional transmission probability of nodes in zone z.
$\pi_{z,s,b}$	Steady state probability of a vehicle in zone z with the backoff time and backoff stage equal to b and s, respectively.
T_{dec}	Time that the backoff time of the tagged node deducts by one.
p_{col}	Collision probability of the tagged node.
p_{suc}	Conditional probability that the in-progress transmission is successful given that the channel is busy.
$p_{\text{suc},z}$	Conditional probability that the in-progress transmission is by a node in zone z, given that the transmission is successful.
$p_{\text{col},z}$	Conditional probability that the in-progress transmission is collided and the longest transmission in the collision is from zone z.
$p_{\text{hcol},z}$	The homogenous collision probability.
$p_{\text{dcol},z}$	The diverse collision probability.
$E[Tx_{\text{suc},z}]$	The mean time of the successful transmission of the tagged node in zone z.
$E[Tx_{\text{col},z}]$	The mean time of the collided transmission of the tagged node in zone z.
$E[T_{\text{suc}}]$	The mean time of the successful in-progress transmission during the backoff of the tagged node.
$E[T_{\text{col}}]$	The mean time of the collided in-progress transmission during the backoff of the tagged node.
$T_{\text{suc},z}$	Successful transmission time of a packet from zone z.
T_{col}	Collision time of the in-progress transmission in the backoff of the tagged node.
s_z	Normalized nodal throughput of vehicles in zone z.
S	Overall throughput of nodes in the system.

adapt CWs according to node transmission rates. By assigning high-rate nodes the relatively small CWs and high-packet transmission probability, the system throughput could be enhanced. Hadaller et al. [14] first consider the performance anomaly in the drive-thru Internet and propose a greedy algorithm where only nodes with the best SNR are allowed to transmit. Unlike [14], in this work, we provide a thorough theoretical study.

3 System Model and Throughput Evaluation

This section details our analytical model for the evaluation of DCF in the highly mobile drive-thru Internet scenario. The many symbols used in this paper have been summarized in Table 1.

3.1 System Model

We consider the drive-thru Internet scenario, as shown in Fig. 1, with nodes connecting to intermittent and serial APs along the road. We focus on the MAC layer under the assumption of perfect channel conditions (i.e., no transmission errors and hidden terminals) with line-of-sight communications. This assumption is typical in literature [7], [15], [11] to evaluate the MAC performance. In this case, the SNR and modulation rates of vehicles are mainly determined by their distance to the AP. Field tests have validated the assumption by showing the strong correlation between distance and transmission rate in vehicular environment [2], [4], [16].

Without loss of generality, we divide the road into multiple spatial zones as shown in Fig. 1. The session outside the coverage of APs is denoted by zone 0. Within the radio coverage of an AP, the road is divided into multiple zones denoted as $\mathbb{Z} = \{1, 2, \ldots, N\}$ such that within each zone z, $z \in \mathbb{Z}$, vehicles have distinct payload transmission rates, denoted by r_z, according to their distance to AP. Let d_z denote the length of each spatial zone $z \in \mathbb{Z}$. With nodes traversing consecutive APs along the road, they are regarded to transit iteratively among the zones in $\mathbb{Z}$. The mobility of vehicles is then represented by the zone transitions using a Markov chain model (inspired by Liu et al. [17]) as shown in Fig. 2 in which each state corresponds to one spatial zone. The time

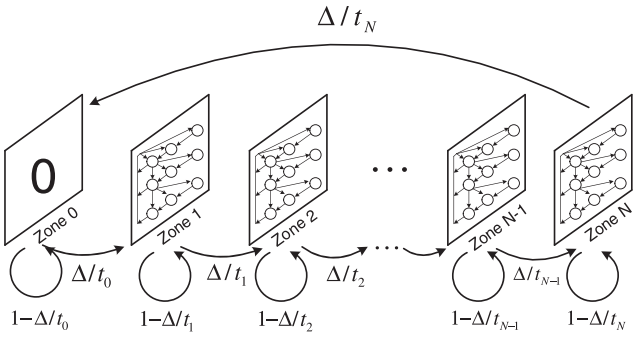

Fig. 2. Three-dimensional Markov model for vehicle nodes.

that nodes stay in each zone $z \in \mathbb{Z}$ is assumed to be geometrically distributed with mean duration of t_z, which is determined by the length of the partition zone and the average velocity, v, of vehicle nodes as $t_z = d_z/v$. As such, within a small duration, e.g., Δ, vehicles either move to the next zone with probability Δ/t_z, or remain in the current zone with the rest probability $1 - \Delta/t_z$. The limiting probability that a node is in zone z at any time is then $d_z/\sum_{n\in\mathbb{Z}} d_n$. With this model, the road could be of multiple bidirectional lanes,[1] and nodes are allowed to have varying speeds but constant mean value.

Within the communication range of APs, packet transmissions are coordinated by the DCF scheme as described in Section 2. We consider the *saturated case* in that each node always has a packet to transmit. The packet length L is assumed to be fixed and same for all the nodes. To address the performance anomaly, we set CW_{min} dependent on the zones such that nodes in different zones transmit with differentiated probabilities. Let W_z denote the CW_{min} of nodes in zone z. Let m denote the maximum number of backoff stage in DCF, which is set to 7 by default in standard [9]. Throughout the work, we assume nodes are homogeneous and abide to the same W_z in zone z. We resist considering the general formulation with service differential to nodes as it could be obtained easily by extending the developed model and, more importantly, it risks making the model difficult to understand.

3.2 Markov Model of Moving Vehicles

To evaluate the DCF performance of individual vehicles, we examine a randomly tagged vehicle and represent its status by a three-dimensional Markov chain $\{Z(t), S(t), B(t)\}$ at time slot t. $Z(t)$ denotes the spatial zone that the node is currently in. $S(t)$ denotes the current backoff stage of the tagged node using DCF. $B(t)$ denotes the backoff time of the tagged node at the current time slot. A discrete and integer scale time is applied, where slot times t and $t+1$ correspond to the beginning of two consecutive backoffs of the tagged node. In other words, the Markov chain is embedded in the countdown of the backoff time. The principle of the three-dimensional Markov chain is sketched in Fig. 2. Similar to [7], it is important to note that this discrete time does not directly map to the real system time; the duration between any two time slots is a random variable as the backoff time of the tagged node could be frozen for a random period.

Fig. 3 plots the state transitions when the tagged node is in zone z. Here, $W_{\max}$ is the maximal W_z among all zones, i.e., $W_{\max} = max\{W_z | z \in \mathbb{Z}\}$. As shown in Fig. 3, upon each transition, the tagged node would have its backoff time deducted by one. Meanwhile, the tagged node would move to the next zone probabilistically based on the mobility model described in the previous section. When the backoff time deducts to zero, the tagged node would initiate one transmission attempt. If the transmission is collided, the tagged node would backoff and selected a new backoff time based on the DCF mechanism as specified in Section 2; otherwise, the backoff stage is cleared to zero. After the transmission attempt, either successful or failed for transmission, the tagged node is possible to move to the next zone and select the backoff time based on the contention window size in the newly arrived zone.

As such, our model is distinct from Bianchi's [7] by considering the node mobility in three aspects. First, after the deduction of the backoff time $B(t)$, the tagged node either stays in the current zone or moves to the next zone with renewed CW_{min} and transmission probabilities. Second, when the tagged node moves to a new zone, its backoff time $B(t)$ reduces smoothly as $B(t) = B(t-1) - 1$, if $B(t-1) \neq 0$, unrelated to zones. Therefore, if $B(t)$ is large, even though the tagged node arrives at a new zone with a very small CW_{min} in the next time slot, it can not benefit immediately. Lastly, the backoff stage is inherited when switching to the next zone with $S(t) = S(t+1)$, if the tagged node does not transmit during the zone transition. In other words, if the tagged node encounters severe collisions, the transmission history will be inherited in the new zone.

Given t_z, $z \in \mathbb{Z}$, the one-step nonnull transition probabilities of the Markov chain from time slot t to $t+1$ are as follows:

1. Arriving at AP (from zone 0 to zone 1):

$$P(1, 0, b|\mathbb{0}) = \frac{E[T_{\text{dec}}]}{t_0 W_1}, \quad b \in [0, W_1 - 1], \tag{1}$$

where $\mathbb{0}$ represents zone 0, and $E[T_{\text{dec}}]$ is the mean duration of one time slot given that the tagged node is not transmitting. $P(1, 0, b|\mathbb{0})$ in (1) accounts for the transition probability that the tagged node moves from zone 0 to zone 1 and selects the backoff time b from the range $[0, W_1 - 1]$. This is because that within one time slot, with probability $E[T_{\text{dec}}]/t_0$, the tagged node move from zone 0 to zone 1 according to the geometrically distributed sojourn time in each zone. After reaching zone 1, the tagged node selects the initial $B(t)$ uniformly from $[0, W_1 - 1]$. As the zone transition and backoff time selection are independent, the overall transmission probability is hence $\frac{E[T_{\text{dec}}]}{t_0 W_1}$. In this work, we turn down the DCF in zone 0—the backoff time set to infinity and the backoff stage cleared to 0—as in this case nodes are out of the transmission range. As such, nodes in zone 0 have only one state whereas those in other zones have multiple states with different values of backoff time and stage.

2. Within the AP coverage (in zones 1 to N): Equation (2) shows the transition probabilities when the tagged node is in the coverage of AP, where p_{col} is the collision probability when the tagged node transmits. $E[Tx_{\text{suc},z}]$ and $E[Tx_{\text{col},z}]$ are

1. Due to the symmetric locations and payload transmission rates of zones along the AP, vehicles along different directions can be modeled using the same Markov chain.

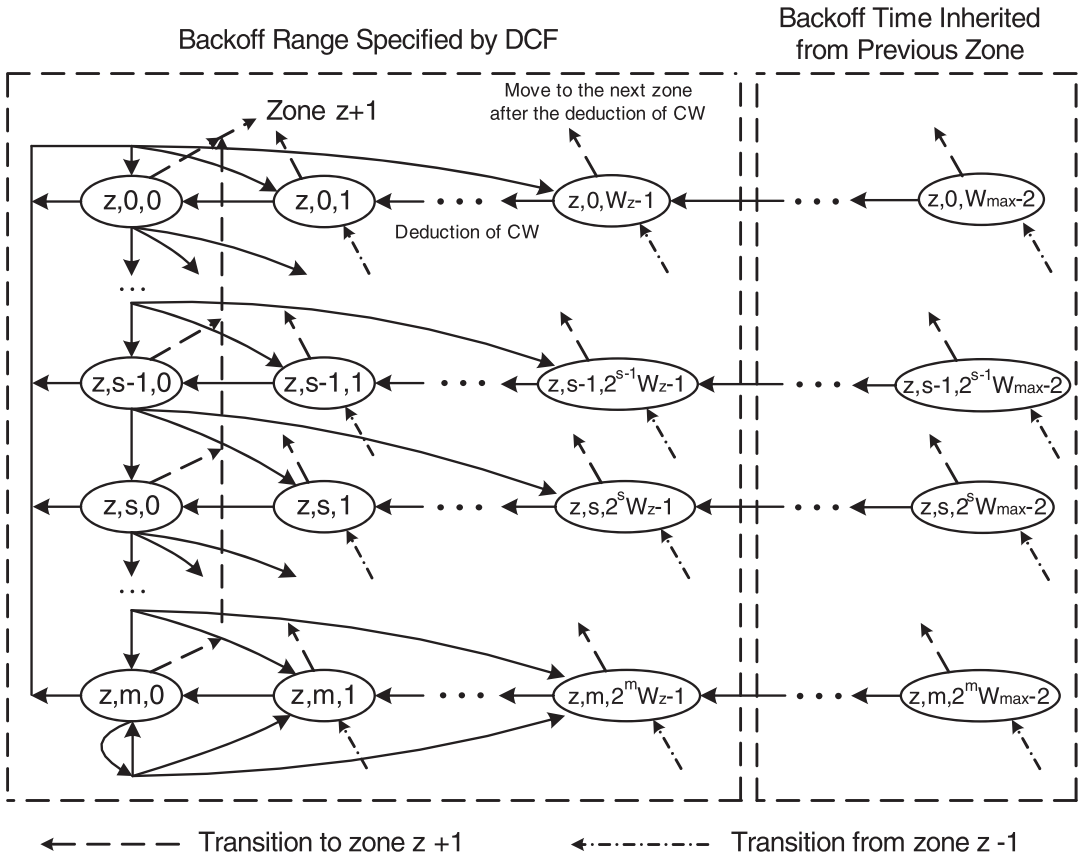

Fig. 3. State space of CW in spatial zone z.

the mean time of one successful and collided transmission of the tagged node in zone z, respectively.

$$P(z,s,b|z,s,b+1)=1-\frac{E[T_{\rm dec}]}{t_z},\quad z\in[1,N],s\in[0,m],b\in[0,2^sW_{\max}-1), \tag{2a}$$

$$P(z,s,b|z-1,s,b+1)=\frac{E[T_{\rm dec}]}{t_{z-1}},\quad z\in[2,N],s\in[0,m],b\in[0,2^sW_{\max}-1), \tag{2b}$$

$$P(z,0,b|z,s,0)=\frac{1-p_{\rm col}}{W_z}\left(1-\frac{E[Tx_{{\rm suc},z}]}{t_z}\right),\quad z\in[1,N],s\in[0,m],b\in[0,W_z-1], \tag{2c}$$

$$P(z,0,b|z-1,s,0)=\frac{1-p_{\rm col}}{W_z}\frac{E[Tx_{{\rm suc},z-1}]}{t_{z-1}},\quad z\in[2,N],s\in[0,m],b\in[0,W_z-1], \tag{2d}$$

$$P(z,s,b|z,s-1,0)=\frac{p_{\rm col}}{2^sW_z}\left(1-\frac{E[Tx_{{\rm col},z}]}{t_z}\right),\quad z\in[1,N],s\in[0,m),b\in[0,2^sW_z-1], \tag{2e}$$

$$P(z,s,b|z-1,s-1,0)=\frac{p_{\rm col}}{2^sW_z}\frac{E[Tx_{{\rm col},z-1}]}{t_{z-1}},\quad z\in[2,N],s\in[0,m),b\in[0,2^sW_z-1], \tag{2f}$$

$$P(z,m,b|z,m,0)=\frac{p_{\rm col}}{2^mW_z}\left(1-\frac{E[Tx_{{\rm col},z}]}{t_z}\right),\quad z\in[1,N],b\in[0,2^mW_z-1], \tag{2g}$$

$$P(z,m,b|z-1,m,0)=\frac{p_{\rm col}}{2^mW_z}\frac{E[Tx_{{\rm col},z-1}]}{t_{z-1}},\quad z\in[2,N],b\in[0,2^mW_z-1]. \tag{2h}$$

$P(z,s,b|z,s,b+1)$ in (2a) accounts for the probability that the tagged node remains in the original zone z after its backoff time deducts by one. $P(z,0,b|z,s,0)$ in (2c) accounts for the probability that the tagged node transmits successfully and starts a new round of backoff. $1-\frac{E[Tx_{{\rm col},z}]}{t_z}$ is the probability that the tagged node remains in the same zone during the collision time. $P(z,s,b|z,s-1,0)$ in (2e) accounts for the probability that the tagged node encounters the collision and backoffs by one stage, all in the original zone. In this scenario, with probability $p_{\rm col}$ that the transmission is collided and with probability $1/2^sW$ that a random backoff interval b is selected within the range $[0,2^sW-1]$. With probability $1-\frac{E[Tx_{{\rm suc},z}]}{t_z}$, the tagged node does not switch zones in this slot time. Equation (2g) shows the transition probabilities when the backoff stage reaches its upper bound m. Equations (2b), (2d), (2f), and (2h) are the transition probabilities that the tagged node moves to the next zone in the new slot time.

3. Departing the AP (from zone N to zone 0)

$$P(\mathbb{0}|N,s,b)=\frac{E[T_{\rm dec}]}{t_N},\quad s\in[0,m],b\in[1,2^sW_{\max}-1], \tag{3a}$$

$$P(\mathbb{0}|N,s,0)=\frac{(1-p_{\text{col}})E[Tx_{\text{suc,N}}]+p_{\text{col}}E[Tx_{\text{col,N}}]}{t_N},\quad s\in[0,m]. \tag{3b}$$

Equation (3) indicates the transition probabilities that the tagged node departs from the zone N and enters zone 0 (out of AP coverage). In these transitions, (3a) is obtained in the same manner of (2a). Equation (3b) accounts for the probability that the tagged node moves out of zone N after it transmits where $(1-p_{\text{col}})E[Tx_{\text{suc,N}}]+p_{\text{col}}E[Tx_{\text{col,N}}]$ is the mean duration of its transmission time.

Let $\pi_{z,s,b}=\lim_{t\to\infty}\Pr\{Z(t)=z,S(t)=s,B(t)=b\}$ be the steady state probability of the Markov chain and $\pi=\{\pi_{z,s,b}\}$ denote the corresponding matrix. Given the state transition probability matrix $\mathbf{P}$ with each nonnull element shown in (1), (2), and (3), $\pi_{z,s,b}$ could be derived with the following balance equations:

$$\begin{cases}\boldsymbol{\pi}\mathbf{P}=\boldsymbol{\pi},\\ \sum_{z=0}^{N}\sum_{s=0}^{m}\sum_{b=0}^{2^sW_{\max}-1}\pi_{z,s,b}=1.\end{cases} \tag{4}$$

3.3 Packet Transmission Time in the Contention

To solve (4), we first consider the expressions of $E[T_{\text{dec}}]$ and $E[Tx_{\text{col},z}]$ and $E[Tx_{\text{suc},z}]$ in (1), (2), and (3).

Let X denote the mean node population in the road segment,[2] excluding the tagged node. Let λ denote the mean arrival rate of nodes to the road segment. According to Little's law

$$X=\lambda\frac{\sum_{z\in\mathbb{Z}}d_z}{v}-1, \tag{5}$$

where $\sum_{z\in\mathbb{Z}}d_z/v$ is the mean sojourn time of nodes in the coverage of AP. Let X_z denote the number of nodes in zone z, excluding the tagged node, then

$$X_z=\frac{Xd_z}{\sum_{n\in\mathbb{Z}}d_n}, \tag{6}$$

where $d_z/\sum_{n\in\mathbb{Z}}d_n$ is the limiting probability that a node is in zone z.

Denote by τ_z the conditional transmission probability given that nodes are in zone z. Mathematically we have

$$\tau_z=\frac{\sum_{s\in[0,m]}\pi_{z,s,0}}{d_z/\sum_{n\in\mathbb{Z}}d_n},\quad z\in\mathbb{Z}. \tag{7}$$

Here, $\sum_{s\in[0,m]}\pi_{z,s,0}$ is the joint probability that a node is in zone z and transmits.

The conditional collision probability p_{col} of the tagged node in (2), given the tagged node is transmitting, is

$$p_{\text{col}}=1-\prod_{z=1}^{N}(1-\tau_z)^{X_z}. \tag{8}$$

3.3.1 Mean Duration of One Time Slot $E[T_{\text{dec}}]$

The mean duration of one time slot $E[T_{\text{dec}}]$, given that the tagged node is not transmitting, is comprised of the unit backoff time δ and mean frozen duration of the backoff time, as

$$E[T_{\text{dec}}]=\delta+p_{\text{suc}}E[T_{\text{suc}}]+(1-p_{\text{suc}})E[T_{\text{col}}], \tag{9}$$

where p_{suc} is the probability that in-progress transmission is successful given that the channel is busy. $E[T_{\text{suc}}]$ and $E[T_{\text{col}}]$ are the mean time of the in-progress transmission with the transmission to be successful and collided, respectively.

$E[T_{\text{suc}}]$ in (9) can be represented as

$$E[T_{\text{suc}}]=\sum_{z\in\mathbb{Z}}p_{\text{suc},z}T_{\text{suc},z}, \tag{10}$$

where $p_{\text{suc},z}$ is the conditional probability that the in-progress transmission is by a node in zone z, given that the transmission is successful. Mathematically

$$p_{\text{suc},z}=\frac{1}{p_{\text{suc}}}X_z\tau_z(1-\tau_z)^{X_z-1}\prod_{n\in\mathbb{Z},n\neq z}(1-\tau_n)^{X_n}. \tag{11}$$

$T_{\text{suc},z}$ in (10) is the successful transmission time when the in-progress transmitting node is in zone z. Mathematically

$$T_{\text{suc},z}=L/r_z+SIFS+ACK/r_z+DIFS+\delta. \tag{12}$$

The collision time T_{col} of the in-progress transmission in (9) equals to the longest transmission time in the collision. Let $p_{\text{col},z}$ denote the probability that the longest transmission time is from nodes in zone z or its mirror zone $z_{\text{mir}}=N+1-z$ along the AP. Here, we jointly consider two zones z and z_{mir} as they have the same distance to AP and payload transmission rate.[3] Similar to [11], $p_{\text{col},z}$ could be computed as

$$p_{\text{col},z}=\begin{cases}\frac{1}{1-p_{\text{suc}}}(p_{\text{hcol},z}+p_{\text{dcol,z}}), & \text{if } z\le\lfloor(N-1)/2\rfloor,\\ \frac{1}{1-p_{\text{suc}}}p_{\text{hcol},z}, & \text{if } z=\lceil N/2\rceil.\end{cases} \tag{13}$$

$p_{\text{hcol},z}$ in (13) is called the homogeneous collision probability representing the probability that only nodes in zones z or z_{mir} transmit, where $z\le\lceil\frac{N}{2}\rceil$. It is shown in (14) which is comprised of three components: 1) the collided nodes are all from zone z; 2) the collided nodes are all from zone z_{mir}; and 3) the collision is from a mixture of nodes from both zones z and z_{mir}.

$$\begin{aligned}p_{\text{hcol},z}=&\big[(1-(1-\tau_z)^{X_z}-X_z\tau_z(1-\tau_z)^{X_z-1})(1-\tau_{z_{\text{mir}}})^{X_{z\text{mir}}}.\\ &+\big(1-(1-\tau_{z_{\text{mir}}})^{X_{z_{\text{mir}}}}-X_{z_{\text{mir}}}\tau_{z_{\text{mir}}}\\ &\quad(1-\tau_{z_{\text{mir}}})^{X_{z_{\text{mir}}}-1}\big)(1-\tau_z)^{X_z}\\ &+(1-(1-\tau_z)^{X_z})(1-(1-\tau_{z_{\text{mir}}})^{X_{z_{\text{mir}}}})\big]\\ &\quad\times\prod_{m=1,m\neq z,m\neq z_{\text{mir}}}^{N}(1-\tau_m)^{X_m},\end{aligned} \tag{14}$$

$p_{\text{dcol,z}}$ in (13) is called diverse collision probability representing the probability that the collision is from at least one node in zones z or z_{mir}, where $z\le\lfloor\frac{N}{2}\rfloor$, and one or more nodes in other zones with larger transmission rate. The expression of $p_{\text{dcol,z}}$ is shown in (15)

2. Each road segment includes the radio coverage of one AP and one zone 0 ahead of it.

3. In case N is odd and $N+1-z=z$, z_{mir} is null with both its population $X_{z_{\text{mir}}}$ and transmission opportunity $\tau_{z_{\text{mir}}}$ to be 0.

$$p_{\mathrm{dcol,z}} = [1-(1-\tau_z)^{X_z}(1-\tau_{z_{\mathrm{mir}}})^{X_{z_{\mathrm{mir}}}}] \left(1-\prod_{m=z+1}^{z_{\mathrm{mir}}-1}(1-\tau_m)^{X_m}\right)\prod_{m=1}^{z-1}(1-\tau_m)^{X_m} \prod_{m=z_{\mathrm{mir}}+1}^{N}(1-\tau_m)^{X_m}. \quad (15)$$

The mean collision time $E[T_{\mathrm{col}}]$ is then

$$E[T_{\mathrm{col}}] = \sum_{z=1}^{\lceil \frac{N}{2} \rceil} T_{\mathrm{col},z} p_{\mathrm{col},z}, \quad (16)$$

where $p_{\mathrm{col},z}$ is obtained in (13). $T_{\mathrm{col},z}$ is the packet collision time in zone z, mathematically

$$T_{\mathrm{col},z} = L/r_z + DIFS + \delta. \quad (17)$$

By substituting (10) and (14) in (9), we can obtain $E[T_{\mathrm{dec}}]$.

3.3.2 Mean Transmission Time $E[Tx_{\mathrm{suc},z}]$ and $E[Tx_{\mathrm{col},z}]$ of the Tagged Node

The successful transmission time $Tx_{\mathrm{suc},z}$ of the tagged node in zone z is deterministic as

$$E\left[Tx_{\mathrm{suc},z}\right] = T_{\mathrm{suc},z}, \quad (18)$$

where $T_{\mathrm{suc},z}$ is specified in (12).

The collision time $Tx_{\mathrm{col},z}$ of the tagged node is a random variable equal to the longest transmission time involved in the collision. Given that one collided node is the tagged node in zone z, the probability that the longest transmission is of nodes from zone z is hence

$$p_{\mathrm{ctag}}, z = \frac{1}{p_{\mathrm{col}}}\prod_{n=1}^{z_{\mathrm{low}}-1}(1-\tau_n)^{X_n}\prod_{n=z_{\mathrm{up}}+1}^{N}(1-\tau_n)^{X_n} \left(1-\prod_{n=z_{\mathrm{low}}}^{z_{\mathrm{up}}}(1-\tau_n)^{X_n}\right), \quad (19)$$

when the collisions nodes are from zones closer to the AP than zones z and z_{mir}, where $z_{\mathrm{mir}} = N - z + 1$, $z_{\mathrm{low}} = \min\{z, z_{\mathrm{mir}}\}$, and $z_{\mathrm{up}} = \max\{z, z_{\mathrm{mir}}\}$. Similar to (14), we jointly consider a zone z and its mirror zone z_{mir} along the AP.

The probability that the longest transmission time is from zone m or its mirror zone $m_{\mathrm{mir}} = N + 1 - m$, where $m < z_{\mathrm{low}}$ and $m_{\mathrm{map}} > z_{\mathrm{up}}$, is

$$p_{\mathrm{ctag,m}} = \frac{1}{p_{\mathrm{col}}}\prod_{n=1}^{m-1}(1-\tau_n)^{X_n}\prod_{n=m_{\mathrm{mir}}+1}^{N}(1-\tau_n)^{X_n} (1-(1-\tau_m)^{X_m}(1-\tau_{m_{\mathrm{mir}}})^{X_{m_{\mathrm{mir}}}}), \quad (20)$$

i.e., nodes in zones farther than zones m and m_{mir} to the AP are not transmitting and at least one node in zones m or m_{mir} transmits.

The mean collision time $E[Tx_{\mathrm{col},z}]$ of the tagged node in zone z is hence

$$E[Tx_{\mathrm{col},z}] = \sum_{n=1}^{z_{\mathrm{low}}-1} T_{\mathrm{col},n} p_{\mathrm{ctag},n} + T_{\mathrm{col},z} p_{\mathrm{ctag},z}, \quad (21)$$

with $T_{\mathrm{col},z}$ given in (17).

3.4 Numerical Solution

By substituting (10), (14), (18), and (21) into (4), the steady state probability of the intermediate states $\pi_{z,s,b}$ could be represented by that of the boundary states $\pi_{z,s,0}$. Therefore, (4) could be managed as a self-contained nonlinear system with unknowns $\pi_{z,s,0}$, where $z \in \mathbb{Z}, s \in [0, m]$, and solved numerically based on the fixed point equation

$$\pi_{z,s,0} = f(\pi_{z,s,0}). \quad (22)$$

As $\pi_{z,s,0} \in [0,1], \forall z \in \mathbb{Z}, s \in [0,m]$, the feasible region of the system $f(\cdot)$ in (22) is a compact convex set. According to the Brouwer's fix point theorem, (22) has at least one solution.

3.5 Derivation of the System Throughput

We evaluate the throughput performance in terms of nodal throughput s_z, representing the throughput achieved by individual node in a given zone z, and the system throughput S, representing the integrated throughput of all the nodes.

The nodal throughput s_z is evaluated as the amount of packet payloads sent by individual node in each transmission in zone z, mathematically

$$s_z = \frac{\tau_z(1-p_{\mathrm{col}})L}{(1-\tau_z)E[T_{\mathrm{dec}}] + \tau_z \times \text{mean trans. time in } z}, \quad (23)$$

where the mean transmission time in z is evaluated as $(1-p_{\mathrm{col}})E[Tx_{\mathrm{suc},z}] + p_{\mathrm{col}}E[Tx_{\mathrm{col},z}]$.

This is because that within one time slot, the tagged node either backoffs or transmits. The former happens with probability $1-\tau_z$. In this case, the channel could be either idle or used by others' transmission with the average duration $E[T_{\mathrm{dec}}]$ specified in (9). The latter happens with probability τ_z. In this case, the transmission of the tagged node could be either successful or failed with mean duration of $(1-p_{\mathrm{col}})E[Tx_{\mathrm{suc},z}] + p_{\mathrm{col}}E[Tx_{\mathrm{col},z}]$. Overall, the denominator in (23) computes the average length of one time slot. Within this duration, the tagged node transmits with probability τ_z and with probability $1-p_{\mathrm{col}}$ the transmission is successful. Upon each successful transmission, an average payload L is delivered.

With X_z nodes transmitting in zone z, the integrated system throughput S of the whole network is

$$S = \sum_{z \in \mathbb{Z}/\{0\}} X_z s_z. \quad (24)$$

3.6 Derivation of Network Size

The throughput characterized by (23) and (24) are dependent on the population of vehicles in each zone. In what follows, we show that the network size could be attained based on the node velocity only.

The mean arrival rate λ to AP and velocity v are in general linearly related as

$$\lambda = n_L k v, \quad (25)$$

where n_L here is the number of lanes in the road segment. k denotes the traffic density corresponding to the number of vehicles per unit distance in each lane along the road segment.

Moreover, based on Greenshield's model [18], the node density k linearly changes with the mean velocity v as

TABLE 2
Parameter of Zones

Zone z	0	1	2	3	4	5	6	7
d_z (m)	20	25	30	40	60	40	30	25
r_z (Mbps)	0	1	2	5.5	11	5.5	2	1
$CW_{\min,z}$	Inf	128	64	32	16	32	64	128

TABLE 3
Default Setting of DCF and Road Traffic Parameters

Time slot δ	$50\mu s$
SIFS	$50\mu s$
DIFS	$128\mu s$
ACK	38 Bytes
Traffic jam density k_{jam}	120 veh/km/lane
Free-way speed v_f	160 km/h

$$k = k_{jam}\left(1 - \frac{v}{v_f}\right), \tag{26}$$

where k_{jam} is the vehicle jam density at which traffic flow comes to a halt. v_f is the free-flow speed corresponding to the speed when the vehicle is driving alone on the road (usually taken as the road's speed limit).

Substituting (25) and (26) into (5), the mean node population in one road segment becomes

$$X = n_L k_{jam}\left(1 - \frac{v}{v_f}\right)\sum_{z\in\mathbb{Z}} d_z - 1, \tag{27}$$

with the tagged node excluded. Accordingly, the mean population in each zone X_z can be computed by substituting (27) into (6).

Given knowledge of n_L, k_{jam}, v_f, and d_z, (27) indicates that the average network size is solely dependent on the velocity v. As a result, vehicles can estimate the achieved throughput via (23) and (24) by measuring its own velocity, and consequently they can conveniently adapt the DCF toward optimized performance which will be discussed in Section 5.

4 Model Validation

4.1 Simulation Setup

We validate our analytical models using simulations based on a discrete event simulator coded in C++. For evaluation purpose, we simulate a drive-thru Internet scenario as shown in Fig. 1, in which an AP is deployed along the road and the vehicles passing through compete for communications using IEEE 802.11b. The whole road segment is divided into 8 zones as specified in Tables 2 and 3, with seven zones in the radio coverage of AP and one zone representing the region outside the coverage of AP. The length and data rates of each zone are based on the extensive measurements reported in [19], also used in [20]. Unless otherwise mentioned, we simulate a road segment composed of eight lanes. Along each lane vehicle nodes are uniformly deployed and moving at the constant velocity $v = 80$ km/h toward the same direction. By default, we set the traffic jam density k_{jam} and the free-way speed v_f as in Table 3 such that there are $X = 130$ vehicles on the road according to (27). Once reaching the end of the road segment, vehicles reenter the road as a new arrival starting from zone 0. Upon each renewal arrival, we clear the transmission history of vehicles with backoff stage set to 0. The vehicles are in the saturated mode with the packet size L of 1,000 Bytes. Parameters of DCF are given in Table 3, which are used for both the simulations and the analysis. In each experiment, we carry out 30 simulation runs and plot the results with the 95 percent confidence interval.

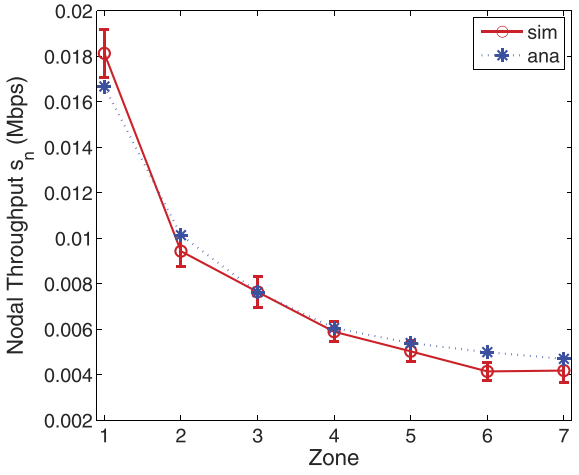

Fig. 4. Nodal throughput s_n with equal contention window ($CW_{min} = 32$) in all zones and other parameters in Tables 2 and 3.

We validate the developed analytical models in two scenarios: 1) equal CW with nodes transmit using the same CW_{min} in all zones, as in legacy IEEE 802.11b [9]; and 2) differentiated CWs where nodes transmit using different CW_{min} values in different zones. In each step, we change the node velocity v and network size X (by tuning k_{jam}) to show the impact of mobility and network size on the throughput performance.

4.2 Equal Contention Window (Legacy IEEE 802.11 DCF)

In this experiment, we set $CW_{min} = 32$ to all zones. In this case, nodes suffer from performance anomaly as described in Section 2 such that their throughput is throttled to the minimum value. This phenomenon is shown in Fig. 4 which plots the nodal throughput s_n in different zones. As we can see, s_n is unrelated with the data rates in different zones. In the meantime, s_n reduces when the zone index increases. This is because that the mean backoff times of nodes increases with the increasing zone index as indicated in Fig. 5a. As a result, the transmission opportunity of nodes reduces with the increasing zone index. The reason for this phenomenon is that in our analytical models and simulations, the backoff stage is reset to 0 when nodes depart from the AP. As a result, the average backoff stage in zone 1 is smaller than that in other zones as in Fig. 5b, and the following zones are also affected due to the mobility.

Fig. 6 shows the throughput performance when node velocity increases from 20 to 140 km/h and $X = 130$ nodes. As can be seen in Fig. 6, both nodal throughput and system

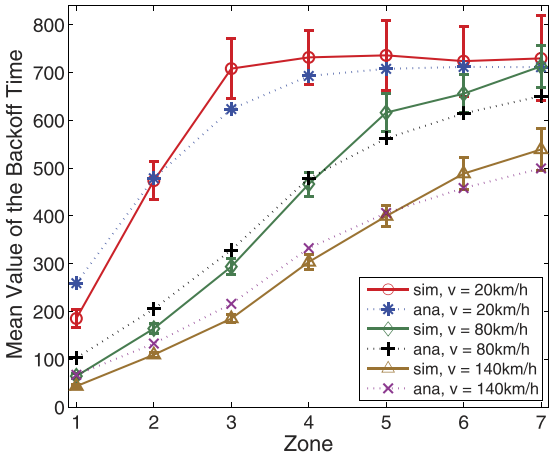

(a) Mean value of backoff time in zone z, computed as $\frac{\sum_{s=0}^{m}\sum_{b=0}^{2^m W_{\max}-1} b\pi_{z,s,b}}{d_z/\sum_{n\in\mathbb{Z}} d_n}$

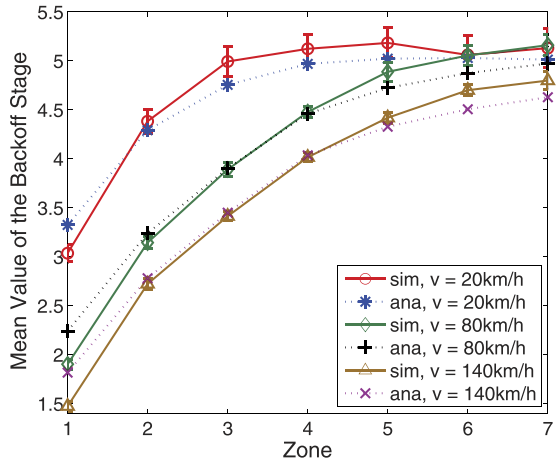

(b) Mean value of backoff stage in zone z, computed as $\frac{\sum_{s=0}^{m}\sum_{b=0}^{2^m W_{\max}-1} s\pi_{z,s,b}}{d_z/\sum_{n\in\mathbb{Z}} d_n}$

Fig. 5. Statistics of backoff time and stage with increasing node velocity, equal contention window ($CW_{min} = 32$) in all zones and constant network size $X = 130$ vehicles.

throughput reduce dramatically when the velocity increases. This is because that with increasing velocity both the mean backoff time and mean backoff stage in each zone reduce as indicated in Fig. 5, resulting in increased collisions shown in Fig. 7. The unintended backoff time is due to the high mobility of nodes. With enhanced mobility, nodes switch zones more often and therefore adapt their contention windows more frequently. As such, the small backoff stage in zone 1 affects the ensuing zones more easily. Despite having the largest transmission rate, nodes in zone 4 encounter the most frequent collisions which results in the large mean backoff time and stages and correspondingly throttles their throughput. The large backoff stage in zone 4 also propagates to the following zones when velocity increases, making the backoff times in $\{5, 6, 7\}$ larger than that in zones $\{1, 2, 3\}$ as shown in Fig. 5.

Fig. 8 shows the impacts of network size on the throughput performance with constant node velocity $v = 80$ km/h. In this experiment, we increase k_{jam} from 40 to 200 veh/km/lane, resulting in the increased network size from 43 to 216 vehicles. As a result, we can see that the system throughput reduces with increased network size. This is because that more intense collisions are encountered with the increasing number of competing nodes.

In summary, deploying equal CW_{min} in different zone would suffer from the performance anomaly. Moreover, the throughput performance is keenly dependent on the network size and node velocity. Increasing the velocity will result in the unintended backoff time distribution and enhanced packet collisions. Therefore, adapting the DCF according to the node velocity is necessary for guaranteed throughput.

4.3 Differentiated Contention Window Sizes among Zones

To address the performance anomaly and boost the system throughput, in this experiment, we let nodes in different zones have different $CW_{\min}$ values and investigate the impacts of network size and velocity on the throughput performance. The $CW_{\min}$ used is shown in Table 2 which is devised based on [9]. The optimal selection of $CW_{\min}$ in different network sizes and node velocities will be discussed in the next section.

Fig. 9 plots the nodal throughput with differentiated contention windows in zones. In this case, as nodes close to AP have relatively smaller CW_{min} and accordingly higher transmission probability, the nodal throughput is a bell-shape curve. Meanwhile, with nodes in front zones having relatively small backoff time as shown in Fig. 10a, the curve tilts to the right.

Fig. 11 shows the throughput performance when node velocity increases. Similar to the equal contention window case, we can see that increasing the velocity also results in the monotonic decreasing of throughput. Moreover, the curve of nodal throughput in Fig. 11a tilts even more severely with the reduced throughput in the back zones. To take a close examine, Fig. 10a shows that mean backoff time changes dramatically when increasing the velocity, while the mean backoff stage changes slightly as shown in Fig. 10b. As we can see, with velocity increasing, both the mean value of backoff time and mean value of backoff stage reduce and they increase as zone index increases. This, on one hand, is because that zone 1 has the smallest mean backoff stage due to the renewal arrival to the AP. With increased velocity, the following zones are also affected from that with the smaller backoff times than expectation. On the other hand, in zone 4, nodes have large backoff stages due to intensive transmissions and collisions. This affects the following zones as shown in Fig. 10b, resulting in large backoff times in those zones. As a direct result of the reduced mean backoff time, the collision probability increases, as shown in Fig. 13, which finally leads to the reduced system throughput as indicated in Fig. 11b. In a nutshell, the high-mobility result in fast transitions between zones which intensively affects the resulting backoff time and the throughput.

In the next experiment, we modify the zone length as specified in Table 2 and examine whether the above

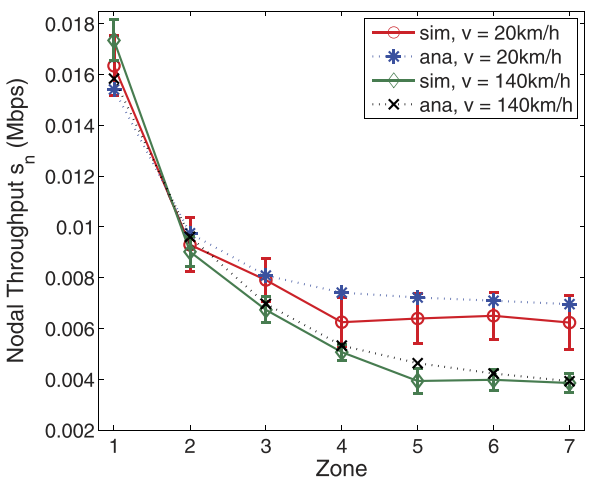

(a) Nodal throughput s_n with increasing velocity

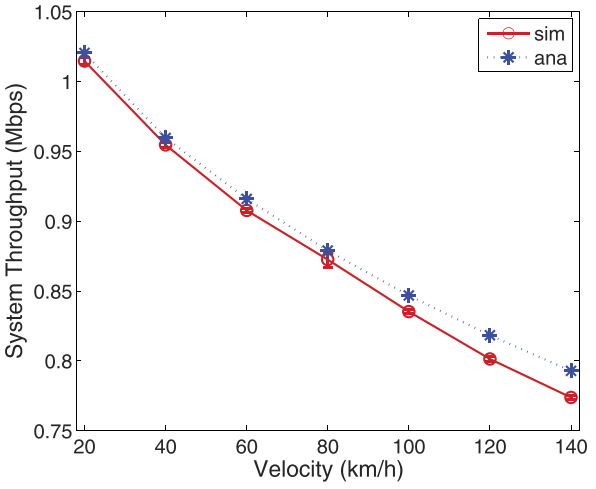

(b) System throughput S with increasing velocity

Fig. 6. Throughput performance with increasing vehicle velocity, equal contention window ($CW_{min} = 32$) in all zones and constant network size $X = 130$ vehicles.

conclusions are still valid when the length of each zone is changed. Fig. 12 plots the throughput performance when the length of each zone is enlarged to four times of the default value in Table 2 while other parameters remain unchanged (as specified in Table 3). As shown in Fig. 12a, when the zone length is enlarged, the nodal throughput is also a bell-shaped curve tilted to right which is similar to that in Fig. 9. With increasing node velocity and fixed node density in Table 3, as indicated in Fig. 12b, the system throughput would also reduce which is similar to that in Fig. 11b. Moreover, as exhibited in Fig. 12, both the nodal throughput and system throughput reduce when the zone length is enlarged. This is because that increasing the zone length implies enlarging the coverage of AP. As the vehicle density remains the same, more vehicles are therefore contending for transmissions, which lead to much severer collisions of transmissions and the degraded throughput performance. Therefore, how to optimally adjust the CW with different road traffic parameters is crucial. Based on our model, we strive to address this issue in the next section of the paper.

Recall that the network size could be estimated based on the node velocity via (27). In the last experiment of this section, we increase the node velocity with fixed k_{jam} and v_f as in Table 3. In this case, the network size adapts with the velocity, which simulates a road segment in different time periods. For example, with low velocity, more nodes are accumulated on the road according to (27), which simulates the busy hour traffic. With high velocity, vehicle traffic on the road is smooth with low density, similar to the late night scenario. As shown in Fig. 14, since both velocity and network size affect the throughput, the resulting throughput is not monotonic when velocity increases. The network achieves the lowest throughput when node velocity is around 80 km/h which happens to be the prevalent speed in the urban freeway.

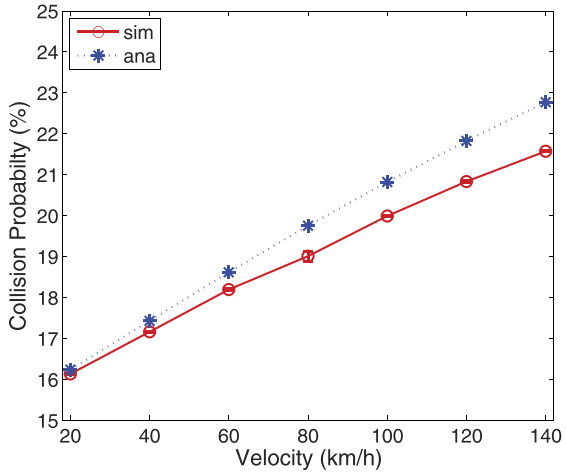

Fig. 7. Packet loss probability with increasing node velocity, equal contention window ($CW_{min} = 32$) in all zones and constant network size ($X = 130$).

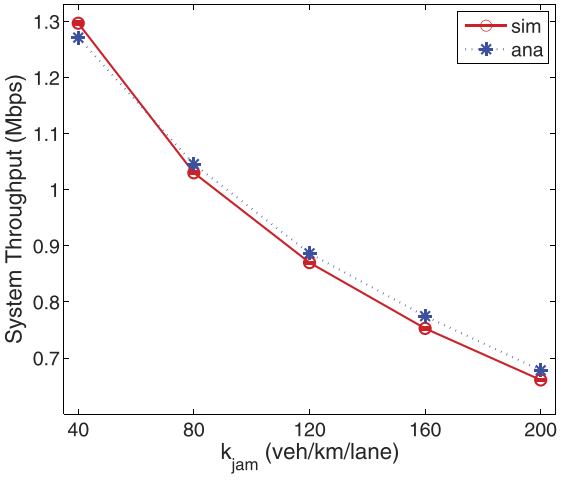

Fig. 8. System throughput when increasing network size (by tuning k_{jam}), equal contention window ($CW_{min} = 32$) in all zones and constant node velocity $v = 80$ km/h.

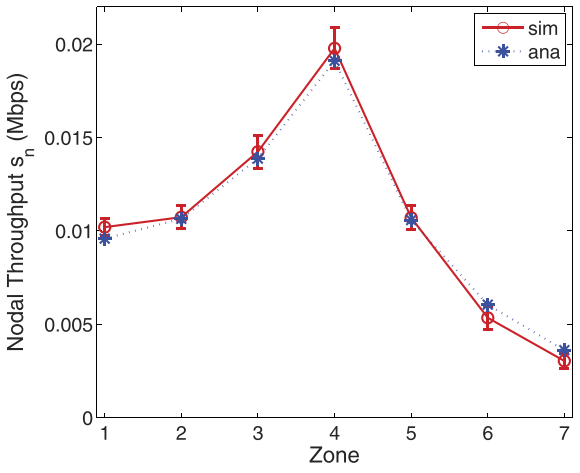

Fig. 9. Nodal throughput s_n with differentiated CW_{min} in zones and other parameters in Tables 2 and 3.

5 Protocol Enhancement

Based on the observations in the previous section, we propose the following assertions as the guideline of the selection of CW_{min} in different zones:

- CW_{min} should adapt to the payload transmission rates of vehicles according to their distance to AP.
- The maximum backoff stage m should be kept small to mitigate the impacts of fast zone transitions on the throughput.
- CW_{min} should adapt to node velocity (and network size).

The reasoning behind the first assertion is obvious: to eliminate the performance anomaly, nodes with different transmission rates should be rendered with different channel access probabilities to fully utilize the transient high-rate connectivity.

The second assertion is rooted in the high mobility of nodes. As indicated in Fig. 11, increasing velocity will reduce the throughput. This is because that in DCF, the value of backoff stage records the transmission history of nodes. With the fast mobility and frequent zone transitions of nodes, the backoff stages in different zones influence each other, resulting in the unintended distribution of backoff times as in Fig. 10. To minimize the mutual interference of backoff times among zones, we should keep m small.

Fig. 15 plots the throughput with $m = 1$ and increasing velocity. The network size is kept constant with $X = 130$ vehicles. "def CW" in Fig. 15 refer to using the default CW_{min} values shown in Table 2. As we can see, increasing the velocity in this case does not affect the throughput much. Instead, the system throughput reduces significantly compared with the value in Fig. 11. This is because that with a smaller m nodes have a smaller backoff time and transmit more frequently with more collisions. Our model is not very accurate when the contention window is small. This is because that in our simulation and the standard, it is possible that a node continually selects the backoff time to be 0 after each transmission and then transmits consecutively. In our analysis, however, we do not take this case into account when computing the slot time $E[T_{\text{dec}}]$ in (9). In real world, the backoff time needs to be large enough to

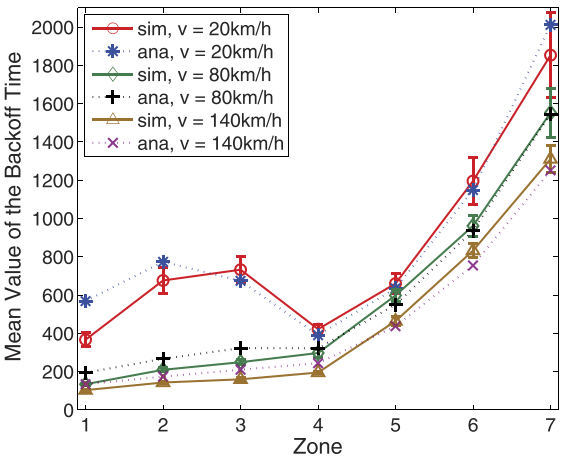

(a) Mean value of backoff time in zone z, computed as $\frac{\sum_{s=0}^{m}\sum_{b=0}^{2^m W_{\max}-1} b\pi_{z,s,b}}{d_z/\sum_{n\in\mathbb{Z}} d_n}$

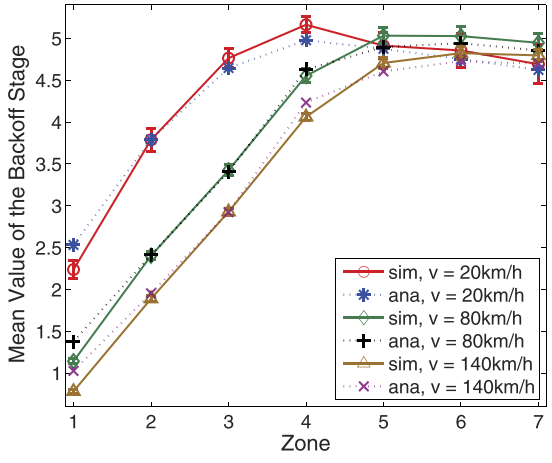

(b) Mean value of backoff stage in zone z, computed as $\frac{\sum_{s=0}^{m}\sum_{b=0}^{2^m W_{\max}-1} s\pi_{z,s,b}}{d_z/\sum_{n\in\mathbb{Z}} d_n}$

Fig. 10. Statistics of backoff time and stage with increasing node velocity, differentiated CW_{min} in zones and constant network size $X = 130$ vehicles.

avoid collisions and consecutive transmissions are rare. Our model is accurate in this case, e.g., when CW is four times of the default CW as shown in Fig. 15. In summary, as indicated in Fig. 15, reducing m would make DCF unscalable and decrease the throughput. To compensate, we could estimate the network size based on the node velocity according to (27), and then adapt CW_{min} accordingly, which explains the third assertion.

Based on the above assertions and provided the node velocity, the optimal $CW_{\min}$ could be obtained by solving the optimization problem as

$$\begin{array}{ll} \underset{W_z}{maxmize} & S \\ s.t., & s_z \geq \eta_z, \quad z \in \mathbb{Z}/\{0\}. \end{array} \tag{28}$$

In (28), the objective is to maximize the system throughput. The constraint dictates that the nodal throughput in different zones must be above certain level. This, on one hand, is to guarantee the throughput fairness of nodes with

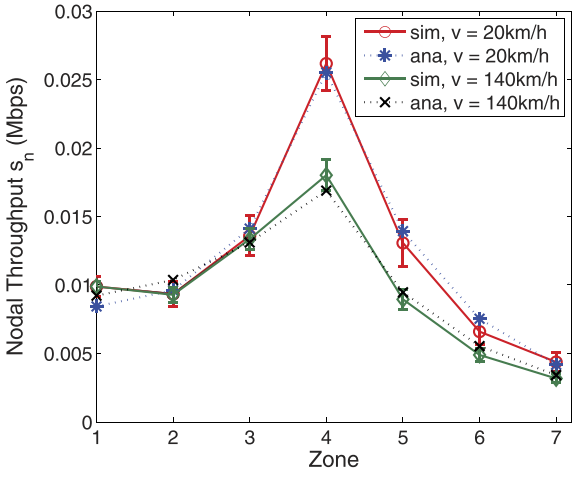

(a) Nodal throughput s_n with increasing velocity

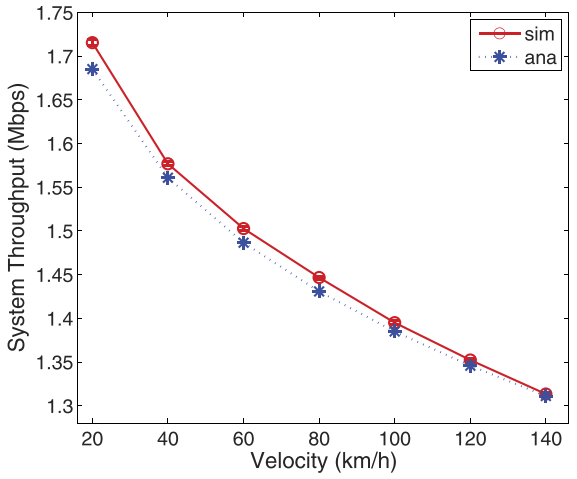

(b) System throughput S with increasing velocity

Fig. 11. Throughput performance with increasing node velocity, differentiated CW_{min} in zones and constant network size $X = 130$ vehicles.

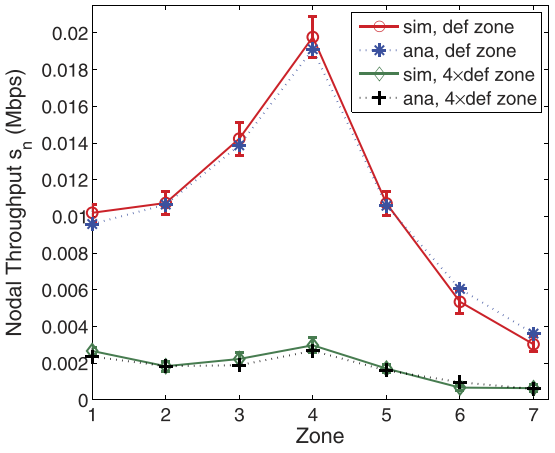

(a) Nodal throughput s_n with constant node velocity $v = 80$ km/h and different zone length

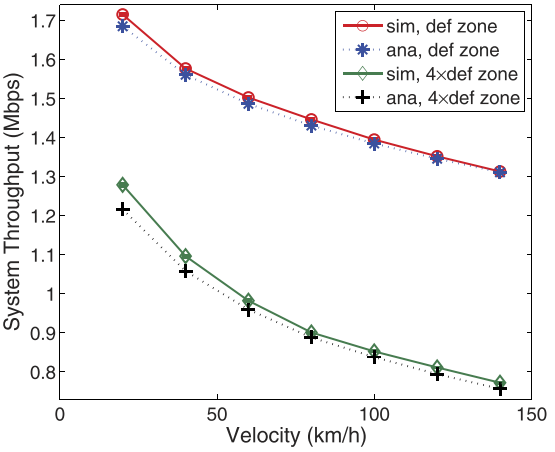

(b) System throughput S with increasing velocities and different zone length

Fig. 12. Throughput performance with different zone length and other parameters in Tables 2 and 3.

different distance to AP. On the other hand, the upper layer applications and protocols may also need guaranteed throughput when nodes are in zones far away from the AP. For example, multimedia applications, e.g., VoIP and live streaming, typically pose a bound on the minimal transmission rate to maintain effective connections [21]. Upper-layer protocols, e.g., TCP, may also require a minimum rate of connection to ensure their functionalities, e.g., congestion control [22].

Equation (28) is an integer programming problem. To reduce the computation complexity, we seek a suboptimal solution as follows: Assuming that the backoff time in different zones are independent with small m (the second assertion). According to (23), we have

$$\frac{s_x}{s_y} \approx \frac{\tau_x}{\tau_y} \approx \frac{W_y}{W_x}. \tag{29}$$

Incorporating (29), the constraint of (31) is satisfied when

$$s_x = \frac{\eta_x}{\eta_y} \times s_y \quad \text{and} \quad s_y \geq \eta_y, \quad x, y \in \mathbb{Z}/\{0\}. \tag{30}$$

As a result, instead of computing W_z in all zones as in (28), we could assume fixed ratios between nodal throughput according to (30), and tune CW_{min} in one zone, e.g., W_1, as

$$\begin{aligned} &\underset{W_1>0}{maxmize} && S \\ &s.t., && W_x = \frac{\eta_x}{\eta_1} \times W_1, \quad x \in \mathbb{Z}/\{0\}, \\ & && s_1 \geq \eta_1, \end{aligned} \tag{31}$$

and adjust W_z in other zone z at the basis of W_1.

Let the ratios of CW_{min} in different zones be same as those in Table 2. Let the setting of simulators be same as those in Table 3, and let m be 1. Fig. 16 plots the optimal value of CW_{min} based on (31) with the increasing velocities (decreasing network size according to (27)). Here, the resultant CW_{min} is represented by W_z^*/W_z^0, $\in \mathbb{Z}/\{0\}$, in which W_z^* denotes the optimal CW_{min} in zone z and W_z^0 is the CW_{min} as specified in Table 2. The system throughput with the optimal CW_{min} is plotted in Fig. 17. Compared with Fig. 14, using the optimal CWs the system throughput can improve for around $15 \sim 45\%$ in different velocities.

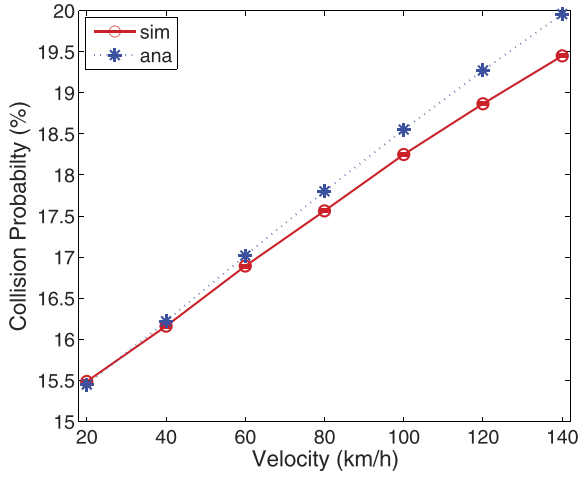

Fig. 13. Collision probability with increasing velocity and adapted network size according to (27) with k_{jam}, v_f in Table 3.

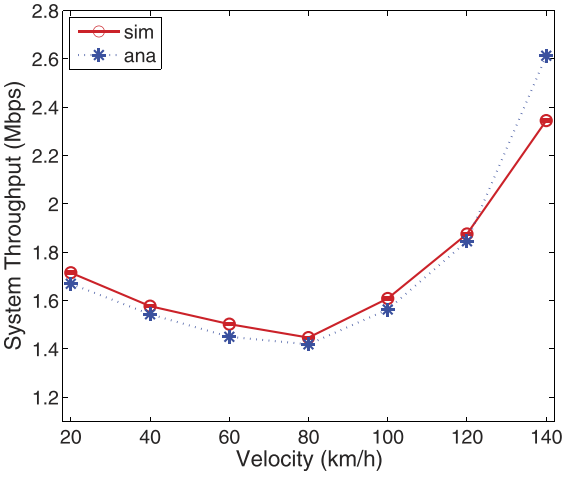

Fig. 14. System throughput with increasing velocity and adapted network size with k_{jam}, v_f in Table 3.

To implement (31), the optimal CWs could be computed offline at different node velocities and then loaded into APs as a table. Based on the estimation of node velocity and network size in (27), APs could search the CW table and apply the optimal CWs correspondingly without much computations. As the network size is random in practice and varying over time [23], the CWs applied also need to be adapted timely. Note that the CW should be adapted slowly, e.g., at the intervals of hours, to capture the changing traffic density in the long term. Moreover, the CW table could be coarse, e.g., mapping the node velocity to appropriate CW at the step of 5 km/h. This avoids the frequent and unnecessary CW adaption and thus make the network unstable.

6 Related Works

In this section, we highlight our contributions in the light of previous works.

Inspired by the pioneer work in [2], the drive-thru Internet has been further investigated in numerous measurement studies from different aspects [3], [4], [24]. While the measurement studies shed insightful lights for the real-world deployments, their focus is mainly on the link quality and transport performance between a vehicle and series of APs passed through. As a result, they do not consider the MAC layer contention when multiple drive-thru vehicles concurrently transmit and compete for the transmission resource. Even with promising link performance as shown in [3], [4], a coarse MAC would result in severe collisions and chaos of transmissions to the connection-limited vehicles; therefore, the elaborate analysis of MAC deserves.

In parallel to the measurement studies, a collection of works are devoted to improve the performance of drive-thru Internet from MAC [25], [26], routing [27], transport [28], and application layer [29]. Zhang et al. [25] proposes a cooperative MAC, namely VC-MAC, for vehicle communications which incorporates the cooperative relays among vehicles with the vehicle to roadside infrastructure communication. By harvesting the spatial and path diversity, VC-MAC significantly improves the throughput and service coverage to volatile fast-moving vehicles. Sikdar [26] devises a reservation-based MAC with the emphasis on

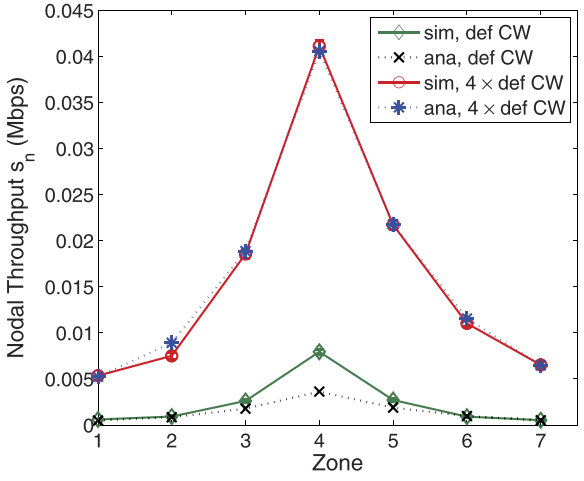

(a) Nodal throughput s_n with $m = 1$ and increasing velocity

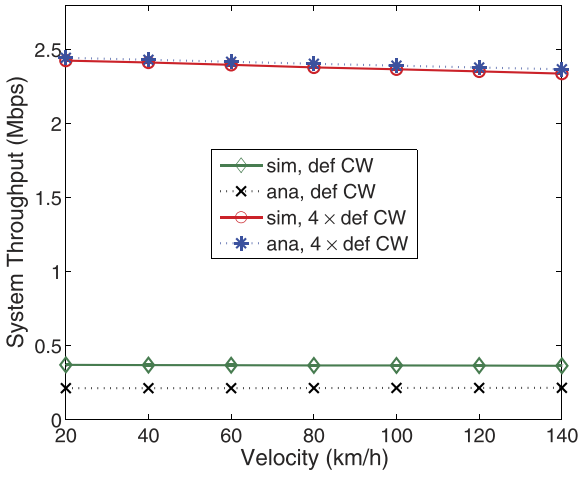

(b) System throughput S with $m = 1$ and increasing velocity

Fig. 15. Throughput performance when $m = 1$ with the constant network size $X = 130$ and increasing velocity.

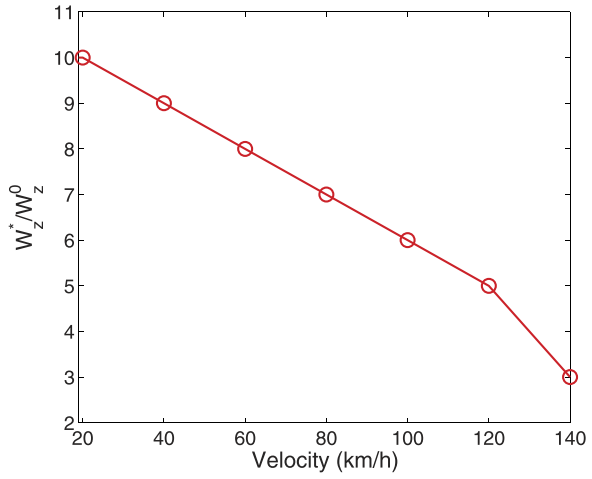

Fig. 16. Optimal CW_{min} with increasing velocity.

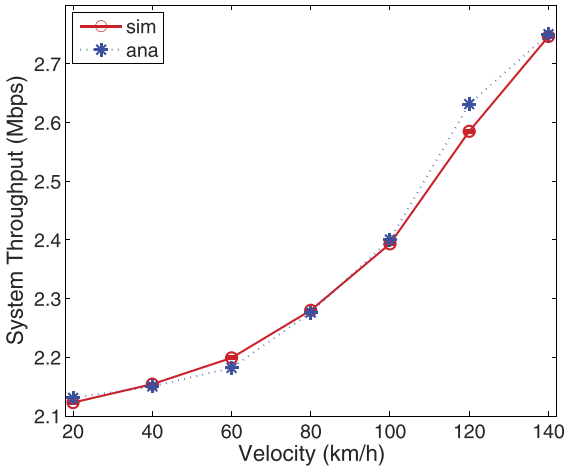

Fig. 17. System throughput with optimal CW_{min} and increasing velocity.

the handoff among APs. Upon the arrival to a new AP, a node first waits for the beacon message from the AP which notifies the available transmission slots to vehicles. After receiving the beacon message, the node then requires to associate with the AP and reserves a time slot for transmission. In contrast to [25], [26], rather than proposing new MAC schemes with distinguished features, we target to an in-depth understanding of the legacy IEEE 802.11 DCF in the newly emerged vehicular environment. The reason is two-fold. First, DCF is the most practical and adopted MAC currently with the broad compatibility to various portable devices in different networks, e.g., hotspot networks in trains and buses [30]. Second, it is widely used in various projects like Fleetnet [31] and DieselNet [27] with proven performance.

On the other hand, some research works focus on investigating the impacts of node mobility on the throughput performance of drive-thru Internet. In [20], Tan et al. develop an analytical model to evaluate the download volume of vehicles per each drive-thru. Assuming the optimal MAC and fair share of airtime, the throughput of each vehicle is computed by averaging the service rate of AP on the population of vehicles. Since the population of vehicles on the road varies over time, the throughput of each node is stochastic and its density function is derived based on a Markov model. Tan et al. [20] consider the network as a flow of nodes. In comparison, our work investigates the throughput from a microscopic view by standing at the viewpoint of individual vehicles. Moreover, unlike [20] which assumes perfect MAC, we model the specific DCF in details and show the quantified impacts of mobility on the MAC throughput.

Furthermore, an extensive body of research has been devoted to the performance evaluation of IEEE 802.11 DCF for WLAN communications [7], [8]. However, as those works mainly focus on the indoor environment with small-scale and static stations, the examine of DCF in the high speed large-scale vehicular environment deserves a fresh treatment. To support the vehicular communications, the IEEE working group has recently proposed IEEE 802.11p [32] as a draft amendment to the IEEE 802.11 standard, namely Wireless Access for Vehicular Environments (WAVE). The new standard adopts IEEE 802.11e EDCF as the MAC. As DCF is the basis of EDCF, our analytical model can be easily extended to study 802.11p. We have considered a simple case in this work to better explain the theory.

7 Conclusion

We conclude this paper by reinforcing our observation that the high mobility of nodes significantly influences the performance of DCF, which results in unintended transmission probabilities rendered to nodes and finally degraded throughput performance. In this work, we have developed an accurate and scalable model to investigate the throughput performance under different velocities and network scales. We have shown that due to the mobility, the network size of the drive-thru Internet is solely dependent on the node velocity, which enables us to optimally configure the DCF by knowing the node velocity only. To enhance the MAC throughput in the drive-thru Internet scenario, we have proposed three assertions as the guideline of the DCF design, which are effective to mitigate the impacts of mobility. As an immediate next step, we plan to further extend our model to evaluate the QoS performance for multimedia applications and the QoS provision schemes in the high-speed drive-thru Internet scenario.

Acknowledgments

This work was supported by the Natural Sciences and Engineering Council (NSERC) of Canada under a Strategic Grant.

References

[1] S. Phillips, "Financial Times: The Future Dashboard," http://specials.ft.com/ftit/june2001/FT3A72I0JNC.html, 2001.
[2] J. Ott and D. Kutscher, "Drive-Thru Internet: IEEE 802.11b for 'Automobile' Users," *Proc. IEEE INFOCOM*, 2004.
[3] V. Bychkovsky, B. Hull, A. Miu, H. Balakrishnan, and S. Madden, "A Measurement Study of Vehicular Internet Access Using in Situ Wi-Fi Networks," *Proc. ACM MobiCom*, 2006.
[4] D. Hadaller, S. Keshav, T. Brecht, and S. Agarwal, "Vehicular Opportunistic Communication under the Microscope," *Proc. ACM MobiSys*, 2007.
[5] P. Bucciol, E. Masala, N. Kawaguchi, K. Takeda, and J. De Martin, "Performance Evaluation of H. 264 Video Streaming over Inter-Vehicular 802.11 Ad Hoc Networks," *Proc. IEEE 16th Int'l Symp. Personal Indoor and Mobile Radio Comm. (PIMRC '05)*, 2005.

[6] J. Angel, "Mercedes-Benz Demos Wireless Network," http://www.allbusiness.com/marketing-advertising/4446481-1.html, 2001.
[7] G. Bianchi, "Performance Analysis of the IEEE 802. 11 Distributed Coordination Function," *IEEE J. Selected Areas in Comm.,* vol. 18, no. 3, pp. 535-547, Mar. 2000.
[8] L.X. Cai, X. Shen, J.W. Mark, L. Cai, and Y. Xiao, "Voice Capacity Analysis of WLAN with Unbalanced Traffic," *IEEE Trans. Vehicular Technology,* vol. 55, no. 3, pp. 752-761, May 2006.
[9] *IEEE Standard 802.11, Part 11: Wireless LAN Medium Access Control (MAC) and Physical Layer (PHY) Specifications,* IEEE, http://standards.ieee.org/getieee802/download/802.11-2007.pdf, 2007.
[10] M. Heusse, F. Rousseau, G. Berger-Sabbatel, and A. Duda, "Performance Anomaly of 802.11b," *Proc. IEEE INFOCOM,* 2003.
[11] D.-Y. Yang, T.-J. Lee, K. Jang, J.-B. Chang, and S. Choi, "Performance Enhancement of Multirate IEEE 802.11 WLANs with Geographically Scattered Stations," *IEEE Trans. Mobile Computing,* vol. 5, no. 7, pp. 906-919, July 2006.
[12] A.V. Babu and L. Jacob, "Fairness Analysis of IEEE 802.11 Multirate Wireless Lans," *IEEE Trans. Vehicular Technology,* vol. 56, no. 5, pp. 3073-3088, Sept. 2007.
[13] T. Joshi, A. Mukherjee, Y. Yoo, and D.P. Agrawal, "Airtime Fairness for IEEE 802.11 Multirate Networks," *IEEE Trans. Mobile Computing,* vol. 7, no. 4, pp. 513-527, Apr. 2008.
[14] D. Hadaller, S. Keshav, and T. Brecht, "MV-MAX: Improving Wireless Infrastructure Access for Multi-Vehicular Communication," *Proc. ACM SIGCOMM Workshop Challenged Networks (CHANTS '06),* 2006.
[15] F. Calì, M. Conti, and E. Gregori, "Dynamic Tuning of the IEEE 802.11 Protocol to Achieve a Theoretical Throughput Limit," *IEEE/ACM Trans. Networking,* vol. 8, no. 6, pp. 785-799, Dec. 2000.
[16] L. Cheng, B.E. Henty, D.D. Stancil, F. Bai, and P. Mudalige, "Mobile Vehicle-to-Vehicle Narrow-Band Channel Measurement and Characterization of the 5.9 GHz Dedicated Short Range Communication (DSRC) Frequency Band," *IEEE J. Selected Areas in Comm.,* vol. 25, no. 8, pp. 1501-1516, Oct. 2007.
[17] K.-H. Liu, X. Shen, R. Zhang, and L. Cai, "Performance Analysis of Distributed Reservation Protocol for UWB-Based WPAN," *IEEE Trans. Vehicular Technology,* vol. 58, no. 2, pp. 902-913, Feb. 2009.
[18] M.A. Chowdhury and A.W. Sadek, *Fundamentals of Intelligent Transportation Systems Planning.* Artech House, 2003.
[19] G. Anastasi, E. Borgia, M. Conti, and E. Gregori, "Wi-fi in Ad Hoc Mode: A Measurement Study," *Proc. IEEE Second Ann. Conf. Pervasive Computing and Comm. (PerCom '04),* 2004.
[20] W.L. Tan, W.C. Lau, O. Yue, and T.H. Hui, "Analytical Models and Performance Evaluation of Drive-thru Internet Systems," *IEEE J. Selected Areas in Comm.,* vol. 29, no. 1, pp. 207-222, Jan. 2011.
[21] B. Yu and C.-Z. Xu, "Admission Control in Roadside Unit Access," *Proc. IEEE 17th Int'l Workshop Quality of Service (IWQoS '09),* 2009.
[22] P. Shankar, T. Nadeem, J. Rosca, and L. Iftode, "CARS: Context-Aware Rate Selection for Vehicular Networks," *Proc. IEEE Int'l Conf. Network Protocols (ICNP '08),* 2008.
[23] F. Bai and B. Krishnamachari, "Spatio-Temporal Variations of Vehicle Traffic in VANETs: Facts and Implications," *Proc. Sixth ACM Int'l Workshop VehiculAr InterNETworking (VANET '09),* 2009.
[24] J. Zhao, T. Arnold, Y. Zhang, and G. Cao, "Extending Drive-thru Data Access By Vehicle-to-Vehicle Relay," *Proc. Fifth ACM Int'l Workshop VehiculAr Inter-NETworking (VANET '08),* 2008.
[25] J. Zhang, Q. Zhang, and W. Jia, "VC-MAC: A Cooperative MAC Protocol in Vehicular Networks," *IEEE Trans. Vehicular Technology,* vol. 58, no. 3, pp. 1561-1571, Mar. 2009.
[26] B. Sikdar, "Characterization and Abatement of the Reassociation Overhead in Vehicle to Roadside Networks," *IEEE Trans. Comm.,* vol. 58, no. 11, pp. 3296-3304, Nov. 2010.
[27] X. Zhang, J. Kurose, B.N. Levine, D. Towsley, and H. Zhang, "Study of a Bus-Based Disruption-Tolerant Network: Mobility Modeling and Impact on Routing," *Proc. ACM MobiCom,* 2007.
[28] J. Ott and D. Kutscher, "A Disconnection-Tolerant Transport for Drive-thru Internet Environments," *Proc. IEEE INFOCOM,* 2005.
[29] Y. Huang, Y. Gao, K. Nahrstedt, and W. He, "Optimizing File Retrieval in Delay-Tolerant Content Distribution Community," *Proc. IEEE 29th Int'l Conf. Distributed Computing Systems,* 2009.
[30] S. Pack, H. Rutagemwa, X. Shen, J.W. Mark, and K. Park, "Proxy-Based Wireless Data Access Algorithms in Mobile Hotspots," *IEEE Trans. Vehicular Technology,* vol. 57, no. 5, pp. 3165-3177, Sept. 2008.
[31] A. Festag, H. Fußler, H. Hartenstein, A. Sarma, and R. Schmitz, "FLEETNET: Bringing Car-to-Car Communication into the Real World," *Computer,* vol. 4, no. L15, p. 16, 2004.
[32] *IEEE P802.11p/D5.0, Draft Amendment to Standard for Information Technology Telecommunications and Information Exchange between Systems LAN/MAN Specific Requirements Part 11: Wireless LAN Medium Access Control (MAC) and Physical Layer (PHY) Specifications: Wireless Access in Vehicular Environments (WAVE),* IEEE, 2008.

Tom H. Luan received the BE degree from Xi'an Jiaotong University, China, in 2004 and the MPhil degree in electronic engineering from the Hong Kong University of Science and Technology, Kowloon, in 2007. He is now working toward the PhD degree at the University of Waterloo, Ontario, Canada. His current research interests focus on wired and wireless multimedia streaming, QoS routing in multihop wireless networks, peer-to-peer streaming, and vehicular network design.

Xinhua Ling received the BEng degree in radio engineering from Southeast University, Nanjing, China, in 1993, the MEng degree in electrical engineering from the National University of Singapore, in 2001, and the PhD degree in electrical and computer engineering from the University of Waterloo, Ontario, Canada, in 2007. He joined Research In Motion in 2007. His general research interests are in the areas of WLAN, WPAN, mesh, cellular networks, and their Internet working, focusing on system architecture, protocol design, and performance analysis.

Xuemin (Sherman) Shen received the BSc degree (1982) from Dalian Maritime University, China, and the MSc (1987) and PhD degrees (1990) from Rutgers University, New Jersey, all in electrical engineering. He is a professor and university research chair, Department of Electrical and Computer Engineering, University of Waterloo, Canada. His research focuses on resource management in interconnected wireless/wired networks, UWB wireless communications networks, wireless network security, wireless body area networks, and vehicular ad hoc and sensor networks. He is a coauthor of three books and has published more than 500 papers and book chapters in wireless communications and networks, control, and filtering. He served as the technical program vommittee chair for IEEE VTC 2010, the symposia chair for IEEE ICC 2010, the tutorial chair for IEEE ICC 2008, the technical program committee chair for IEEE GlobeCom 2007, the general cochair for Chinacom 2007 and QShine 2006, and the founding chair for the IEEE Communications Society Technical Committee on P2P Communications and Networking. He also served as a founding area editor for the *IEEE Transactions on Wireless Communications*; editor-in-chief for *Peer-to-Peer Networking and Application*; associate editor for the *IEEE Transactions on Vehicular Technology*, *Computer Networks*, and *ACM Wireless Networks*; and guest editor for *IEEE JSAC*, *IEEE Wireless Communications*, *IEEE Communications Magazine*, and A*CM Mobile Networks and Applications*. He received the Excellent Graduate Supervision Award in 2006, the Outstanding Performance Award in 2004 and 2008 from the University of Waterloo, the Premier's Research Excellence Award (PREA) in 2003 from the Province of Ontario, Canada, and the Distinguished Performance Award in 2002 and 2007 from the Faculty of Engineering, University of Waterloo. He is a registered professional engineer of Ontario, Canada, a fellow of the IEEE, an Engineering Institute of Canada Fellow, and a Distinguished Lecturer of IEEE Communications Society.